

Phenomenological investigation of many-body induced modifications to the one-dimensional density of states of long quantum wires

This article has been downloaded from IOPscience. Please scroll down to see the full text article.

2008 J. Phys.: Condens. Matter 20 164209

(<http://iopscience.iop.org/0953-8984/20/16/164209>)

View [the table of contents for this issue](#), or go to the [journal homepage](#) for more

Download details:

IP Address: 129.252.86.83

The article was downloaded on 29/05/2010 at 11:30

Please note that [terms and conditions apply](#).

Phenomenological investigation of many-body induced modifications to the one-dimensional density of states of long quantum wires

T Morimoto¹, N Yumoto¹, Y Ujiie¹, N Aoki¹, J P Bird² and Y Ochiai¹

¹ Graduate School of Advanced Integration Science, Chiba University, 1-33 Yayoi-cho, Inage-ku, Chiba 263-8522, Japan

² Department of Electrical Engineering, University at Buffalo, The State University of New York, Buffalo, NY 14260-1920, USA

Received 16 October 2007, in final form 14 November 2007

Published 1 April 2008

Online at stacks.iop.org/JPhysCM/20/164209

Abstract

We investigate the behavior of interacting one-dimensional systems using linear (close to equilibrium) and non-linear transport measurements of split-gate quantum wires of varying channel length. Our measurements reveal a remarkable resonance effect in the differential conductance, which exhibits a pronounced peak, for a narrow range of source–drain voltage, at the transition from tunneling to open transport. This peak becomes more pronounced with increase of channel length, but is rapidly suppressed by increase of temperature or (in-plane) magnetic field. We believe that these unique features may arise from the dependence of transport on the electron density of states, and suggest a phenomenological model to account for this transport behavior.

(Some figures in this article are in colour only in the electronic version)

1. Introduction

The investigation of ballistic transport in one-dimensional (1D) systems has been started from the discovery of quantization of their conductance as step-features in unit of $2e^2/h$ [1, 2]. This phenomenon is well understood by the single-particle notation of the Landauer formula, which predicts that the conductance in 1D should depend only on the number of occupied subbands. On the other hand, one other unique property of 1D systems concerns the form of their density of states (DOS), which exhibits van Hove singularities due to the opening of each subband. The experiment of scanning ‘tunneling’ spectroscopy for 1D carbon nano-tube clearly shows this kind DOS by the differential conductance measurement [3]. In the case of *open* (i.e. not tunneling) transport phenomena, however, the energy dependence of the 1D DOS is well known to be canceled by that of the electron group velocity. In other word, the large contributions on currents from ‘large group velocity’ electrons are trade-off with their ‘small 1D DOS’. This is one important reason of appearance of ‘step-like’ quantized conductance.

Research on *interacting* 1D systems started well before the discovery of the 1D conductance quantization, with the pioneering theoretical studies of Tomonaga and Luttinger [4, 5]. The strictly one-dimensional, strongly confined, carrier system that these authors considered have come to be referred to as the Tomonaga–Luttinger liquid (TLL). This unique system exhibits strong modifications to its momentum distribution function, reflecting the role of long-range interactions and the breakdown of the quasi-particle description. The characteristic feature of the TLL is that it exhibits a power-law dependence on various physical parameters, under conditions of low-energy excitation. The experimental observation of this power-law behavior was first provided in studies of the temperature-dependent conductance of semiconductor quantum wires (QWs) at zero magnetic field [6] and in the fractional-quantum-Hall regime [7, 8]. More recently, detection of the TLL state has been reported in photoemission studies of single-walled carbon nanotubes, which function as naturally-formed one-dimensional conductors [9], by measuring the energy of

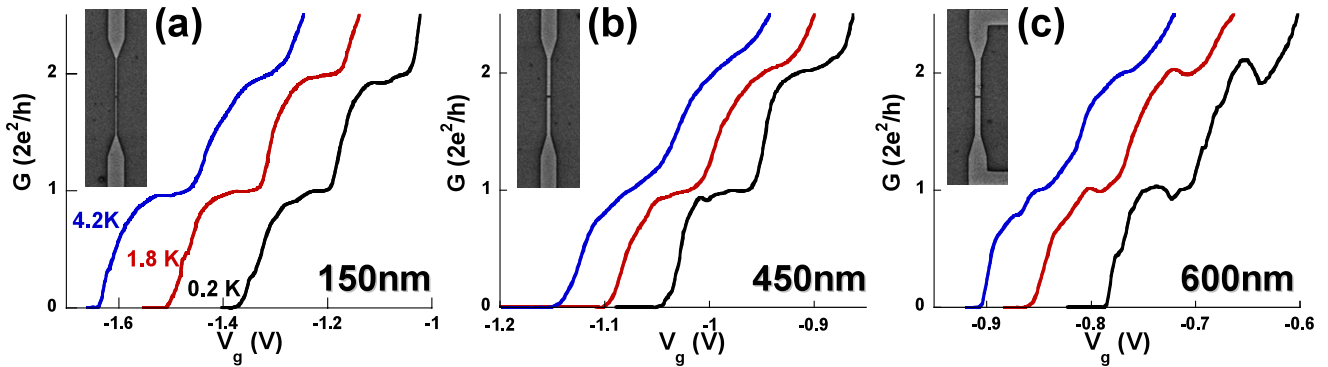


Figure 1. Main-panel: the quantized conductance of the three QWs at different temperatures: 4.2 K (left), 1.8 K (middle) and 0.2 K (right). The curves have been shifted by: 150 nm: 0.1 V for 1.8 K, 450 nm: 0.1 V for 4.2 K, 600 nm: 0.05 V for 1.8 K and 0.1 V for 0.2 K. Insets: scanning electron micrographs of the QW gate patterns.

electrons ejected from their states. Such results indicate that the TLL is truly an important phenomenon in real systems, in spite of the purely theoretical models that were used to construct the main results of TLL theory in the 1950s.

In addition to evidence of TLL behavior, other many-body effects have also been discovered in QWs during the last decade or so. The realization of the significance of the *0.7 feature* [10] provides one of the most important examples of this work, as demonstrated by the diverse group of papers that are collected together for this special issue. These studies suggest that this phenomenon may be related to a spontaneous (either *static* or *dynamic*) spin polarization of carriers in the 1D channel, in the limit where the carrier density is about to vanish. In the dynamical picture of spin polarization, a quantum-dot (QD) like feature is believed to form in the self-consistent potential of the QW, leading to the realization of a bound state that can localize a single spin [11, 12]. According to this model, a Kondo effect, caused by the dynamically-localized spin moment, is believed to be responsible for the smearing of the 0.7 feature near zero bias at low temperatures [13, 14]. There have been many studies [15–27] that have investigated the dependence of the 0.7 feature on parameters including temperature, magnetic field, carrier density, channel length, confinement potential, and the nature of the geometrical connections of the QW to its reservoirs. Most recently, we have provided evidence for the formation of a bound state near pinch-off, using coupled quantum point contacts to detect the resulting spin localization [28]. In spite of this progress, however, the microscopic origins of this phenomenon remain unclear, suggesting that new experimental approaches to this problem are needed to clarify this issue.

In this paper, we describe another effect that appears in the conductance of QWs, in the same low-density regime in which other many-body effects are observed. Unlike the 0.7 feature, the manifestations of many-body interactions that we discuss are present under strong non-linear conditions. Specifically, we find that the differential conductance of our QWs shows a strong resonant enhancement over a narrow range of the source–drain voltage (V_{sd}), an effect that becomes more pronounced as the length of the QW is increased [29]. Based

on a detailed analysis of the linear and differential conductance of these QWs, we suggest a phenomenological model for our observations in which transport should be dependent on the manifested 1D DOS as proportional to $C \times (1/E^n)$, here C is constant as $C > 1$ and n is index as $n > 0.5$, by many-body effect in low carrier densities, when the reservoirs align with the band edge of ground state after formation of energy gap near zero bias voltages.

2. Sample preparation and measurement setup

QWs of different length (150-, 450- and 600 nm) were realized in the two-dimensional electron gas (2DEG) of a modulation-doped GaAs/AlGaAs heterostructure, by applying a gate voltage (V_g) to split gates (see figure 1) on the top surface of the same Hall-bar mesa. We note here the lithographic pattern of these gates, which consists of a uniform channel of constant width without any deliberate adiabatic connection to the 2DEG reservoirs. The 2DEG was located 75 nm below the top surface of the heterostructure and had a density of $2.1 \times 10^{11} \text{ cm}^{-2}$ and a mobility of $1.1 \times 10^6 \text{ cm}^2 \text{ V}^{-1} \text{ s}^{-1}$ (both at 4.2 K). The split gates were separated from each other by a lateral distance of $20 \mu\text{m}$, significantly longer than the mean-free path of the 2DEG ($9.1 \mu\text{m}$). Using this multi-QW device, we can therefore make meaningful comparisons of the length dependence of the transport properties, while avoiding substrate-dependent variations of behavior. Electrical measurements of the linear conductance (we denote this conductance as $G(V_g)$) were performed using the sufficient small ac excitation ($30 \mu\text{V rms}$) from a lock-in amplifier, while combined ac + dc excitation was used for direct measurements of the differential conductance dI/dV_{sd} (denoted as $g(V_{sd})$ for fixed V_g , or $g(V_g)$ for fixed V_{sd}). The differential conductance represents the local slope of the I – V curve at each applied V_{sd} . Consequently, the linear and differential conductance differ in the case where the I – V curve exhibits any non-linear form. The sample was mounted in the mixture of a dilution refrigerator and the measurement temperature was varied from 0.2 to 13 K. Magnetic field could also be applied in the same plane as the 2DEG substrate.

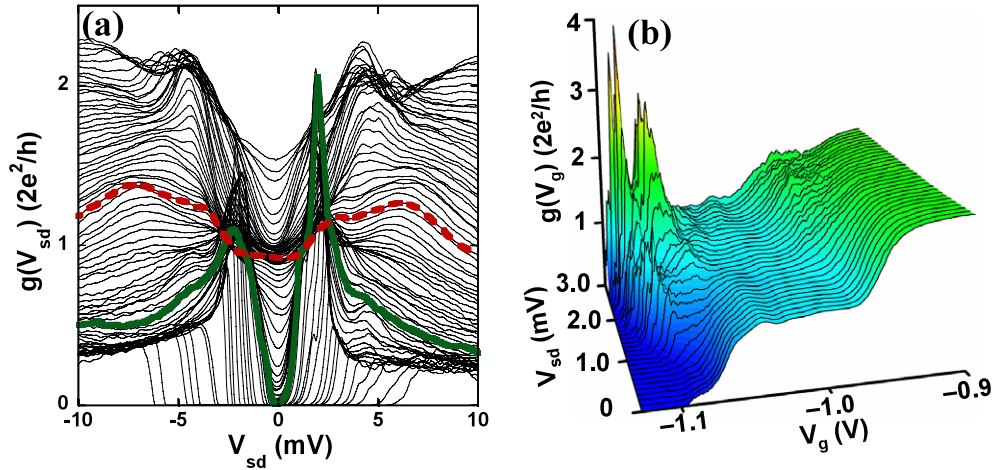


Figure 2. (a) $g(V_{sd})$ of the 450 nm QW at 0.2 K. Each curve corresponds to differential conductance measured for fixed V_{sd} . The solid and dashed bold curves are discussed in the text. (b) The three-dimensional plot of $g(V_g)$ with 0.1 mV steps in V_{sd} bias.

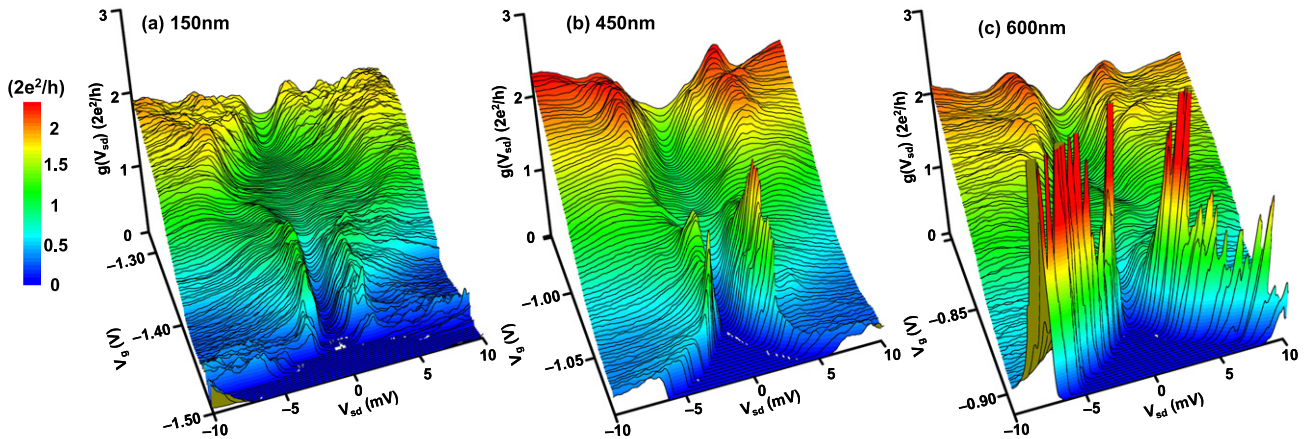


Figure 3. Three-dimensional plots of $g(V_{sd})$ of the (a) 150 nm, (b) 450 nm, and (c) 600 nm QWs with 2.0- (150- and 450 nm) and 1.5 mV (600 nm) steps in V_g .

3. Experiment results

The quantized linear conductance of the different QWs (with zero dc bias) is shown at several temperatures in figure 1. At the lowest temperature (0.2 K), the conductance steps are well resolved due to the suppression of thermal smearing. While these steps are weakened with increasing temperature, the 0.7 feature becomes more clearly resolved in the 450- and 600 nm QWs. The robustness against increase of temperature should be related to the energy level spacing due to lateral confinement, at the bottleneck in the potential profile [19]. The temperature insensitivity of the conductance steps in the 150 nm QW therefore likely comes from a large energy spacing due to a steep parabolic potential. (This is also consistent with the stability of the conductance plateaus as V_{sd} is varied; as we will show in figure 3, the 150 nm device exhibits a large stable plateau in this differential conductance.) The 450- and 600 nm wires show weak conductance fluctuations that are thought to be caused by quantum interference and impurity scattering [30]. All of these results are consistent with previous

reports by other groups on transport in ballistic and weakly-disordered wires.

Rather than the linear conductance, the differential conductance plays an important role in this study, by providing detailed information on the internal microscopic state of the QWs. It is known quite generally that the differential conductance provides information on the DOS of conductors. In the discussion of linear transport in one-dimensional conductors, as mentioned already, the energy dependence of the DOS is canceled by that in the group velocity when calculating the channel current. This cancellation is also thought to extend to the discussion of non-linear transport, in which the finite bias present can cause unequal populations of the one-dimensional subbands by the source and drain, leading to the observation of so-called ‘half plateaus’ [31, 32]. Consequently, the differential conductance is a powerful tool for investigating the reservoir-induced filling of energy levels in one-dimensional systems. To illustrate this, figure 2(a) shows $g(V_{sd})$ for the 450 nm wire at 0.2 K, and at a series of different gate voltages (2.0 mV steps). At $V_{sd} = 0$ V, these curves show a bunching at $2e^2/h$ that corresponds to the

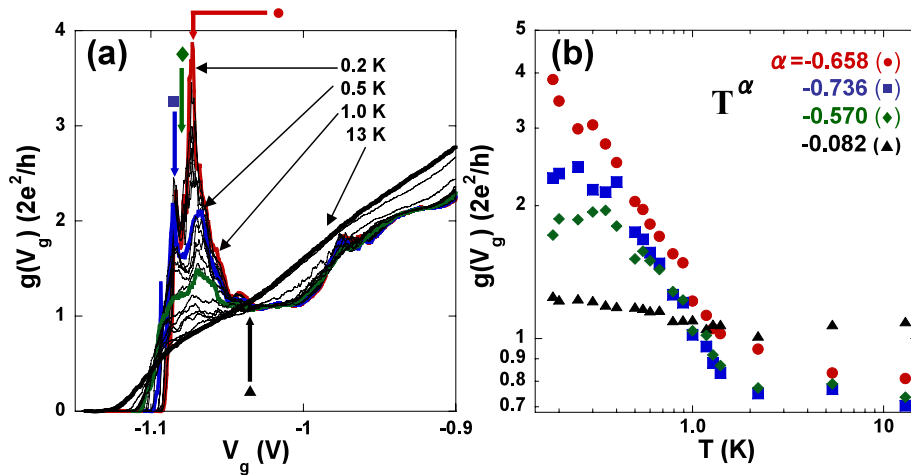


Figure 4. (a) The temperature dependence of the $g(V_g)$ peaks in the 450 nm QW, measured for a source–drain bias of $V_{sd} = 2.2$ mV and for a change of temperature from 0.2 to 13 K. The thick colored curves correspond to 0.2 K, 0.5 K, 1.0 K, and 13 K from high to low gV_g , respectively. The arrows with symbols indicate the gate voltage of each plotted in (b). (b) The temperature dependence of the differential conductance at the gate voltages denoted by the corresponding symbols in (a). The power-law indexes of each data set are indicated at the top of the figure.

conductance plateau observed at a similar value in the linear conductance (see figure 1). Very different behavior is seen at finite V_{sd} , however, where there are two roughly-symmetric peaks that rise rapidly to a value significantly exceeding $2e^2/h$. In the clearest manifestation of this behavior, as indicated by the solid bold curve in the figure, one of these peaks exceeds $2 \times 2e^2/h$, even though the zero- V_{sd} conductance is completely pinched-off. With increase of the zero- V_{sd} conductance, however, the resonances are rapidly suppressed (see the dashed bold curve).

For more detailed information on the unusual resonant behavior noted in figure 2(a), it is helpful to represent $g(V_g)$ as a three-dimensional contour. Figure 2(b) shows such a contour for the 450 nm QW, which was constructed by incrementing V_{sd} in 0.1 mV steps. From this contour, we see that $g(V_g)$ does not change much as the dc bias is increased from 0 to 0.7 mV. At 0.8 mV, however, an additional shoulder-like structure is formed close to pinch-off. This structure grows with further increase of $g(V_g)$, ultimately splitting into two pronounced peaks whose amplitude can be seen to approach $4 \times 2e^2/h$ in this slow sweep. In addition to these two peaks, at the high-bias end of the contour, we can also clearly observe what appear to be weak, higher order, replicas of this effect, which smear the half plateau at $1.5 \times 2e^2/h$.

The $g(V_{sd})$ spectra of the three different QWs are shown in figure 3. The flat part of the center region in each plot corresponds to the expected integer plateau at $2e^2/h$. The 150 nm QW shows this region most clearly, which is consistent with the robustness of the linear conductance to temperature noted in figure 1. With regards to the resonant peaks at finite V_{sd} , these exhibit a clear evolution, becoming more pronounced with increase of the channel length. In the case of the 600 nm wire, the resonant peaks exceed $3 \times 2e^2/h$. Consistently, for all three QWs, however, the resonant peaks appear at the transition between pinch-off and the onset of open conduction. In the case of the 450 nm wire, it is clear that applying large V_{sd} (in excess of a few mV) suppresses

the resonances, and that no additional resonances are observed either when the gate confinement is increased beyond pinch-off. Since the effect of both of these variations will tend to be to introduce distortions, or asymmetries, in the confining potential of the QW, they may suppress the one-dimensional character of the wires. On the other hand, the 600 nm wire shows the resonant peaks much more robustly, which may reflect the fact that the 1D channel is more well defined in this longer device. The suggestion of these results (length dependence and sensitivity to V_g and V_{sd}) therefore seems to be that the 1D electron confinement plays a critical role in giving rise to this resonance phenomenon.

To obtain further information on the origins of the resonant peaks, we have measured their temperature (T) dependence at fixed V_{sd} . Figure 4(a) shows the evolution of $g(V_g)$ for the 450 nm wire ($V_{sd} = 2.2$ mV), as the temperature is varied from 0.2 to 13 K. The peaks show a sensitive temperature dependence, decreasing quickly as the temperature is increased. They eventually disappear around 2 K, while the quantized conductance plateaus only vanish around 13 K (figure 4(b)). To express this behavior more quantitatively, we have chosen the points indicated by the arrows with associated symbols in figure 4(a), and plotted the temperature dependence of the conductance at these gate voltages. These four points correspond to the main peak (circles), the second peak (squares), a point intermediate between both peaks (diamonds), and a background point away from these resonances (triangles). The quantitative temperature dependence at all four of these gate voltages corresponds well to a power-law variation, at least away from saturated regions at both ends of the temperature range. For the data represented by circles, squares and diamonds, the index of the power-law variation appears to be quite similar, at least within the experimental uncertainty. An average of the index obtained for these three points yields 0.65 ± 0.09 , clearly distinct from the much lower index describing the variation of the background conductance. Although we have not measured

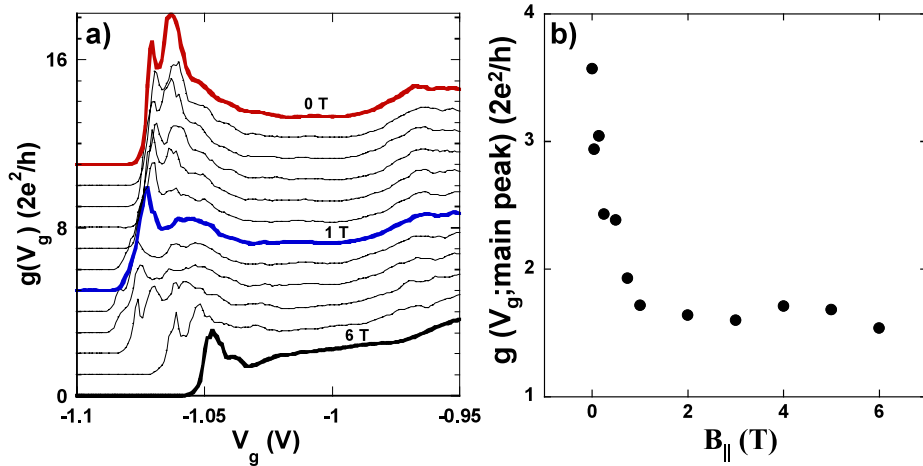


Figure 5. (a) The in-plane magnetic-field dependence of the differential conductance for the 450 nm QW at a source–drain voltage of 2.4 mV and at 0.2 K. The different curves correspond to 0, 0.05, 0.15, 0.25, 0.5, 0.75, 1, 2, 3, 4, 5, and 6 T. (b) The in-plane magnetic-field dependence of the peak height for the largest peak at 0 T.

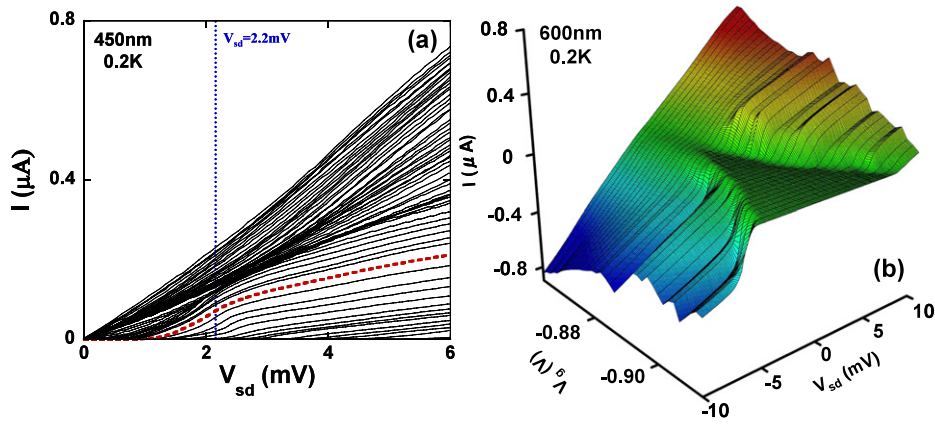


Figure 6. (a) The I – V characteristics of the 450 nm QW for various fixed gate voltages at 0.2 K. The dotted curve corresponds to the case where the peak in the differential conductance is clearly developed. (b) A three-dimensional plot of the I – V characteristics of the 600 nm QW at 0.2 K. The flat regions around zero bias voltage correspond to the pinch-off regime, and the regions of steeply-increasing current that bound this regime yield the strong peaks in the differential conductance.

the temperature dependence for the 600 nm in detail, we expect that the resonances exhibited by this device should exhibit a larger power index since its resonances are clearly very much larger than those exhibited by the 450 nm QW (figure 3).

Application of a magnetic field in the same plane as the 2DEG should induce a Zeeman energy shift, without giving rise to any cyclotron force. The response of the resonant peaks to such a magnetic field is shown in figure 5(a), in which the field is increased from 0 to 6 T. We focus here on the magnetic-field dependence of same peak investigated in our temperature-dependent studies. This peak is rapidly suppressed with application of the magnetic field, as we show quantitatively in figure 5(b). Our results reveal a parabolic shift of the pinch-off condition at high magnetic fields, which is likely a manifestation of the well-known diamagnetic shift of the 2DEG two-dimensional subband-edge [33]. We also note the appearance and disappearance of sub-peaks as a function of the magnetic field. The origin for these features is not clear at present and further investigations are needed to fully understand the influence of the magnetic field.

4. Discussions and conclusions

We believe that an important key to understanding the resonance phenomenon we have described is to connect it to the local slopes that appear in the source–drain current–voltage (I – V) characteristics of the QWs. In figure 6(a), we show these characteristics for the 450 nm wire, for the range of V_g corresponding to the transition from pinch-off to beyond the $2e^2/h$ plateau in the linear conductance. The bunching of curves indicates this quantized plateau, while the constant slope seen for all curves at higher bias corresponds to the half plateau (at e^2/h) in the differential conductance. In addition, several curves can be seen with a steep slope near 2 mV (as we indicate using the dashed bold curve in figure 6(a)). The temperature dependence shown in figure 4 corresponds exactly to the variation of the local slope in each curve at $V_{sd} = 2.2$ mV (dotted line in figure 6(a)). The differential conductance peaks correspond to these steep regions and in the 600 nm wire these regions are more clearly resolved. This can be seen in the contour plot for this device in figure 6(b). The flat part of the

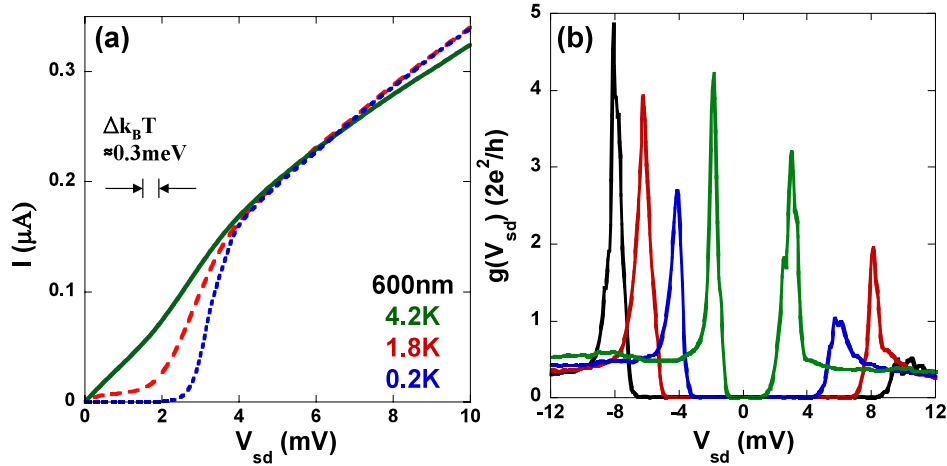


Figure 7. (a) The temperature dependence of the I - V characteristic of the 600 nm wire at fixed gate voltage. The different temperatures are indicated with the bold (4.2 K), dashed (1.8 K) and dotted (0.2 K) curves. The energy scale corresponding to a change of thermal energy from 4.2- to 0.2 K is indicated on the figure. (b) The selected peaks for comparison the line shapes. These have asymmetric line shape similar the 1D DOS in both sides V_{sd} .

contour corresponds to the pinch-off regime, which is bounded on both sides by steep regions that yield the sharp peaks in the differential conductance.

The temperature dependence of the I - V characteristics indicates more clearly the essence of the resonance phenomenon, as we indicate in figure 7(a). The three curves in this figure were measured for fixed gate voltage, at 4.2 (bold line), 1.8 (dashed line) and 0.2 K (dotted line). At higher biases, the current becomes independent of temperature and all three curves fall on top of each other, indicating that in this limit the current flowing through the wire is determined by the applied bias. At lower biases, however, the line shape is sensitive to decrease of temperature. This low-temperature behavior contains two significant features, one of which is the steep feature mentioned above, and the other of which is the apparent opening of an energy gap near zero bias, as revealed by the strong suppression of current.

The existence of steep features in I - V characteristics, due to the opening of an energy gap, is well known from the field of superconductivity, in particular from the study of tunneling in superconductor/insulator/normal metal junctions. This phenomenon can be understood as arising from quasi-particle tunneling from the Fermi surface of the normal metal, to the superconducting state, via the huge DOS that exists at the edge of the energy gap. In this situation, the differential conductance directly reflects the resonance in the DOS. Although this system is of completely different origin to the one that we study, we nonetheless suggest that the steep increase of current that we observe is also caused by the onset of transport via the large DOS of the confined 1D system. This idea is supported by the asymmetric line shape of $g(V_{sd})$, which exhibits considerable similarity with the non-interacting 1D DOS as shown in figure 7(b). In this picture, as the gate voltage is varied from pinch-off towards the onset of conduction, the electrochemical potential of the biased reservoir firstly reaches the lower edge of 1D DOS and generates the large resonance reflected singularity of DOS. With increase of the applied bias, the resonance then gradually decreases, following the

decrease of the DOS and yielding the asymmetric resonance line shapes. Although we cannot conclusively justify this speculation, we nonetheless believe that the large resonant peaks, exceeding $2e^2/h$, and the channel-length dependence of this effect, support an interpretation in terms of the 1D DOS.

It is particularly important to emphasize here that the size of the gap, which we can infer to be nearly 3 meV from the 0.2 K data in figure 7(a), is much larger than the thermal energy available at 4.2 K (~ 0.3 meV as shown in figure 7(a)). This indicates that the effect of decreasing temperature is more than to simply decrease the thermal broadening. To understand the additional effect of temperature, a comparison of the linear conductance at two very different temperatures, and the contour map of figure 3(b), are shown together in figures 8(a) and (b). Figure 8(a) shows that reducing temperature decreases the smearing of the linear conductance lineshape, consistent with findings in previous studies [10, 13, 15, 19, 23]. Indeed, the higher conductance regions show fixed crossing points at $1.5 \times 2e^2/h$ and $2.5 \times 2e^2/h$. The lowest fixed point is, however, displaced significantly from its expected value at $0.5 \times 2e^2/h$, indicating that the low-temperature conductance is suppressed near the pinch-off region. We can see this effect more clearly in the 2D contour plot of $g(V_{sd}, V_g)$ in figure 8(b). In figures 8(c)-(h) we show schematic images of the energy diagrams for the various points indicated in figure 8(b). The $2e^2/h$ integer plateau in the differential conductance corresponds roughly to the diamond-shaped region enclosed by the dashed lines (e.g. [13, 19, 31]). The flattest portion of this region occurs at $V_g \sim -1.01$ V, and the dashed line diamond in figure 8(b) is centered at this gate voltage. The contour plot shows that the conductance near zero bias does not vary symmetrically inside of this region, but is rapidly suppressed when the gate voltage is made more negative than -1.01 V. The contour shows that the conductance is completely suppressed for the band alignment corresponding to that of figure 8(d). We also note in the contour plot how it is possible to draw (dotted) lines from the pinch-off condition at higher source-drain bias, which intersect the vertex of the abovementioned

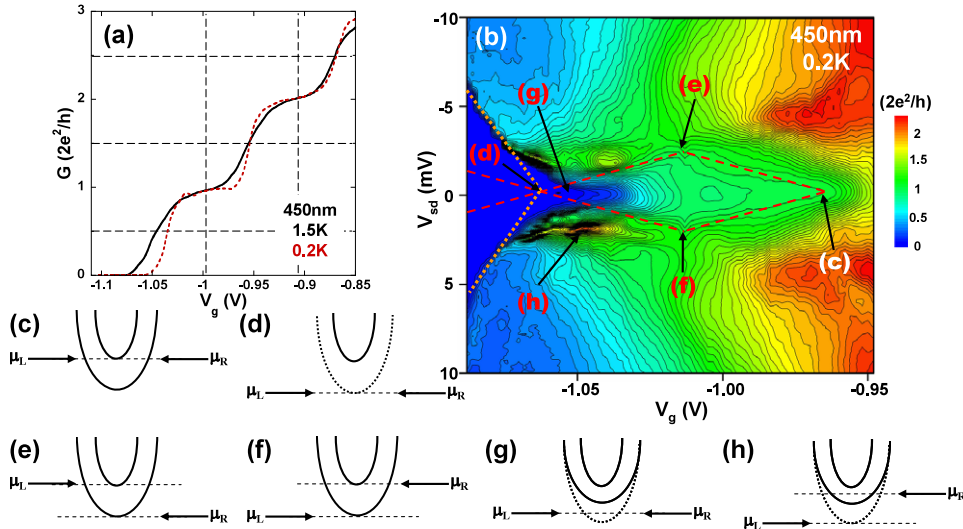


Figure 8. (a) A comparison of the linear conductance of the 450 nm QW at 1.5- and 0.2 K. The horizontal grid lines indicate the values of 1.5- and $2.5 \times 2e^2/h$ and the vertical lines indicate the crossing points of the two-different temperature curves. The 1.5 K is shifted to $+0.02$ V. (b) Contour plot of $g(V_{sd})$ as a function of V_g and V_{sd} , measured in the 450 nm at 0.2 K (figure 3(b)). The diamond shape formed by the dashed lines represents the extrapolated shape expected for the integer plateau at $2e^2/h$ in the absence of the resonance features. The dotted lines are linear extrapolations that are drawn from the left vertex of the diamond-shaped area and which follow the boundary of the pinch-off region. (c)–(h) Schematic pictures showing the energy of the 1D channel and the reservoirs for each point indicated in the main panel of (b).

diamond at $V_{sd} = 0$ V. In this sense, we see that the rapidly suppressed conductance close to the vertex of the diamond corresponds to the appearance of a gap that is larger than the thermal energy as shown in figure 8(g) (the conductance drops to zero several meV faster than we would expect from the extrapolations based on the dotted lines). The steep increase in the I – V curves, and the corresponding differential conductance peaks, are observed when one reservoir aligns with the energy state modified by the formation of the energy gap as shown in figure 8(h).

We believe that standard single-particle notions of transport are insufficient to account for the unusual behavior that we have reported here. It is, of course, well known that tunneling via impurity sites, or accidentally-formed QDs, can give rise to conductance resonances in QWs whose properties are determined by the Coulomb blockade of transport [34–39]. The amplitude of the resulting Coulomb resonances (or oscillations) as gate voltage is varied typically much smaller than what we observe in our experiment, however. The formation of such unintentional QDs typically furthermore results in the observation of a series of quasi-regular Coulomb oscillations, while we always only observe a single resonance as the gate voltage is swept at fixed V_{sd} . Moreover, the Coulomb resonances are seen in the *linear* conductance of the QWs, in marked contrast to the behavior found here. To further discount the possibility of some unintentional impurity effect, we have also investigated how asymmetric gate biasing (e.g. $V_g = -1.8$ and -0.4 V applied on the 450 nm wire) influences the resonances, and find their characteristics to be unaffected by this in all asymmetric measurement. As a further indication that the resonance phenomenon which we observe does not result from simple Coulomb charging, we note that the zero bias peak in the differential conductance

of unintentional QDs is typically symmetric [39], something which we never observe for our resonance. While non-linear transport via QD states can be well understood in terms of the contributions from resonant tunneling and inelastic processes, it is difficult to apply such concepts to explain the strong resonant enhancement of the differential conductance reported here. Transport via higher two-dimensional subbands of the electron gas can also be ruled out as the origin of the resonance phenomenon [40, 41]. If the peaks did indeed correspond to the process of populating such higher levels, the conductance should exhibit quantized plateaus in integer units of $2e^2/h$. It is clear in figure 3, however, that the conductance shows plateaus at 1- and $2 \times 2e^2/h$, even when the resonance is seen near the onset of conduction. Finally, we note that simple quantum interference, or other scattering, processes should not have the effect of enhancing the conductance beyond the quantized value at finite bias.

While the origin of the resonant features that we observe remains to be resolved, we can identify their important phenomenological properties. (1) The effect is enhanced in longer channels and at lower temperatures. This indicates that one-dimensional phenomena may play an important role in giving rise to the resonances. (2) The peaks in the differential conductance originate from the presence of regions with steep slopes in the I – V characteristics. These strong enhancements of current should be caused by transport via the large singularity in the 1D DOS. (3) The strongly suppressed current at lower temperatures indicates the opening of an energy gap near zero bias in the pinch-off region. This energy gap is clearly signified by an additional suppression of the zero bias conductance near pinch-off at low temperature. The conductance resonances appear at both sides of this gap structure. If the energy gap arose from a simple

shift of the subbands to higher energy, the temperature-dependent I - V curves should not merge in the higher bias range. Therefore, we should consider that the formation of an energy gap is responsible for the manifestation of DOS structure in the conductance resonances. (4) The power-law temperature dependence, as well as the magnetic-field dependence, indicates a strong sensitivity to environmental fields. These facts also support the possibility of the 1D interaction as the origin, possibly involving spin on the basis of the magnetic-field behavior.

Here, we wish to suggest a speculative model to account for the unusual non-linear transport behavior we observe in experiment. In this model, we consider that electrons near the band edge of the 'original' ground state are shifted and redistributed to a higher energy level formed by the appearance of the energy gap. Due to conservation of the total number of states, the resulting DOS should have a larger value near the band bottom than that expected from the usual free-electron form ($1/E^{0.5}$). We therefore suggest that the DOS in this region can be described as C/E^n , where the constant $C > 1$ and the index $n > 0.5$. When conduction occurs via this modified DOS, the current should be proportion to $1/E^{(n-0.5)}$ and so should exhibit a singularity at the band edge. The inferred energy gap formation, and the strong differential conductance peaks observed in experiment, can be understood within this phenomenological model. As to the origin of this phenomenon, there are several possibilities associated with different mechanisms. In the case of the repulsive TLL state, it is possible that the conductance near pinch-off is suppressed and that this could give rise to power-law temperature-dependent variations of the conductance. Previous investigations of the TLL state in 1D systems have focused on the manifestations of such power-law behavior in the quantized conductance steps. In our experiment, the channel-length dependence of the resonances is consistent with the fact that the interaction strength depends on the channel length. Other possible mechanisms, however, are the formation of a spin gap or an insulating state. The energy gap of a 1D Heisenberg anti-ferromagnet chain, having integer spin ($S = 1$), is well known as the Haldane gap [42]. More recently, a striking transition from a conducting to an insulating state has been reported, and related to the possible formation of a Wigner crystal or a charge-density wave [43]. The formation of an energy gap, or some insulating state, are also considered to be reasonable candidates to explain our results, although more investigations are needed to conclusively determine the origins of the behavior we observe.

In conclusion, we have observed a strong resonant-peak structure in the differential conductance of long quantum wires under non-linear conditions. The peaks appear to reflect an energy-dependent transition in the wire at low temperatures. Our observations appear consistent with the opening of a gap in the electronic spectrum at low temperatures, which is manifest directly in the temperature-dependent I - V characteristics. The differential conductance resonances having a 1D-DOS like line shape may arise from a breakdown of the cancelation of the 1D DOS in the subband currents. The appropriate theoretical description of these remarkable and unique transport features

should account for the detailed phenomenological features mentioned above. Since we are unaware of prior reports of this phenomenon, these results should be important to understanding the role of electron interactions in 1D systems.

Acknowledgments

This work was supported in part by Grants-in-Aid for Scientific Research of the Japan Society for the Promotion of Science (JPSJ) No. 19204030. T Morimoto was also supported by a JSPS Research Fellowship.

References

- [1] van Wees B J, van Houten H, Beenakker C W J, Williamson J G, Kouwenhoven L P and van der Marel D 1988 *Phys. Rev. Lett.* **60** 848
- [2] Wharam D A, Thornton T J, Newbury R, Pepper M, Ahmed H, Frost J E F, Hasko D G, Peacock D C, Ritchie D A and Jones G A C 1988 *J. Phys. C: Solid State Phys.* **21** L209
- [3] Wildoer Jeroen W G, Venema Liesbeth C, Rinzler Andrew G, Smalley Richard E and Dekker C 1998 *Nature* **391** 59
- [4] Tomonaga S 1950 *Prog. Theor. Phys.* **5** 544
- [5] Luttinger J M 1963 *J. Math. Phys.* **4** 1154
- [6] Tarucha S, Honda T and Saku T 1995 *Solid State Commun.* **94** 413
- [7] Wen X G 1990 *Phys. Rev. B* **41** 12838
- [8] Miliken F P, Umbach C P and Webb R A 1995 *Solid State Commun.* **97** 309
- [9] Ishii H *et al* 2003 *Nature* **426** 540
- [10] Thomas K J, Nicholls J T, Simmons M Y, Pepper M, Mace D R and Ritchie D A 1996 *Phys. Rev. Lett.* **77** 135
- [11] Hirose K, Meir Y and Wingreen N S 2003 *Phys. Rev. Lett.* **90** 026804
- [12] Rejec T and Meir Y 2006 *Nature* **442** 900
- [13] Cronenwett S M, Lynch H J, Goldhaber-Gordon D, Kouwenhoven L P, Marcus C M, Hirose K, Wingreen N S and Umansky V 2002 *Phys. Rev. Lett.* **88** 226805
- [14] Meir Y, Hirose K and Wingreen N S 2002 *Phys. Rev. Lett.* **89** 196802
- [15] Reilly D J *et al* 2001 *Phys. Rev. B* **63** 121311
- [16] Reilly D J, Buehler T M, O'Brien J L, Hamilton A R, Dzurak A S, Clark R G, Kane B E, Pfeiffer L N and West K W 2002 *Phys. Rev. Lett.* **89** 246801
- [17] Reilly D J 2005 *Phys. Rev. B* **72** 033309
- [18] Kristensen A *et al* 1998 *Physica B* **180** 249
- [19] Kristensen A *et al* 2000 *Phys. Rev. B* **62** 10950
- [20] de Picciotto R, Pfeiffer L N, Baldwin K W and West K W 2005 *Phys. Rev. B* **72** 033319
- [21] DiCarlo L, Zhang Y, McClure D T, Reilly D J, Marcus C M, Pfeiffer L N and West K W 2006 *Phys. Rev. Lett.* **97** 036810
- [22] Rokhinson L P, Pfeiffer L N and West K W 2006 *Phys. Rev. Lett.* **96** 156602
- [23] Crook R, Prance J, Thomas K J, Chorley S J, Farrer I, Ritchie D A, Pepper M and Smith C G 2006 *Science* **312** 1359
- [24] Bruus H, Cheianov V V and Flensberg K 2001 *Physica E* **10** 97
- [25] Tokura Y and Khaetskii A 2002 *Physica E* **12** 711
- [26] Wang C K and Berggren K-F 1996 *Phys. Rev. B* **54** R14257
- [27] Berggren K-F, Jaksch P and Yakimenko I 2005 *Phys. Rev. B* **71** 115303
- [28] Yoon Y, Mouroukh L, Morimoto T, Aoki N, Ochiai Y, Reno J L and Bird J P 2007 *Phys. Rev. Lett.* **99** 136805

- [29] Morimoto T, Henmi M, Naito R, Tsubaki K, Aoki N, Bird J P and Ochiai Y 2006 *Phys. Rev. Lett.* **97** 096801
- [30] Nixon J A, Davies J H and Baranger H U 1991 *Phys. Rev. B* **43** 12638
- [31] Patel N K *et al* 1990 *J. Phys.: Condens. Matter* **2** 7247
- [32] Patel N K, Nicholls J T, Martin-Moreno L, Pepper M, Frost J E F, Ritchie D A and Jones G A C 1991 *Phys. Rev. B* **44** 13594
- [33] Rinaldi R, Cingolani R, Lepore M, Ferrara M, Catalano I M, Rossi F, Rota L, Molinari E and Lugli P 1994 *Phys. Rev. Lett.* **73** 2899
- [34] Scott-Thomas J H F, Field S B, Kastner M A, Smith H I and Antoniadis D A 1989 *Phys. Rev. Lett.* **62** 583
- [35] van Houten H and Beenakker C W J 1989 *Phys. Rev. Lett.* **63** 1893
- [36] Weis J, Haug R J, Klitzing K v and Ploog K 1992 *Phys. Rev. B* **46** 12837
- [37] Tang Y S, Davies J H, Williamson J G and Wilkinson C D W 1992 *Phys. Rev. B* **45** 13799
- [38] Staring A A M, van Houten H and Beenakker C W J 1992 *Phys. Rev. B* **45** 9222
- [39] Moser J, Roddaro S, Schuh D, Bichler M, Pellegrini V and Grayson M 2006 *Phys. Rev. B* **74** 193307
- [40] Salis G, Heinzl T, Ensslin K, Homan O J, Bachtold W, Maranowski K and Gossard A C 1999 *Phys. Rev. B* **60** 7756
- [41] Apetrii G, Fischer S F, Kunze U, Schuh D and Abstreiter G 2004 *Physica E* **22** 398
- [42] Haldane F D M 1983 *Phys. Rev. Lett.* **50** 1153
- [43] Thomas K J, Sawkey D L, Pepper M, Tribe W R, Farrer I, Simmons M Y and Ritchie D A 2004 *J. Phys.: Condens. Matter* **16** L279